NIR Photodetector Based on Nanosecond Laser-Modified Silicon

Ji-Hong Zhao, Chun-Hao Li, Xian-Bin Li, Qi-Dai Chen,
Zhan-Guo Chen, and Hong-Bo Sun, *Fellow, IEEE*

Abstract— A crystalline silicon (Si) surface was modified using nanosecond laser pulses in an argon atmosphere. The laser-modified Si (M-Si) samples have a higher performance and thermostable absorption in the broadband range (400–2400 nm) than conventional Si. The concentration of carrier electrons in the M-Si layer is at least five orders of magnitude greater than the carrier concentration of the Si substrate. Using the N^+–N^- junction formed between the M-Si layer and the Si substrate, visible and near-infrared (VIS-NIR) M-Si photodetectors are made. The N^+–N^- photodiode has good rectification characteristics and a high photoresponse to the subbandgap NIR light at 1310 nm. At the same time, the M-Si photodetector at a low reverse bias shows a large gain to the VIS-NIR light above the bandgap. By comparing the response time of the M-Si photodetector to the light of 900 and 1310 nm, the response speed of the device to the photon above-bandgap energy is faster.

Index Terms— Absorption, nanosecond (ns) laser, near-infrared (NIR) photodetector, silicon (Si).

I. INTRODUCTION

SILICON (Si)-BASED infrared photodetectors are the key component of Si-based optoelectronic integration technologies [1]–[7]. However, photodetector-based crystalline Si has no photoresponse to infrared light longer than 1.1 μm due to its inherent band structure. In recent years, extending the absorption limit of crystalline Si using pulsed laser modification as an effective method has been adopted by many researchers [8]–[17]. Generally, below-bandgap absorption of pulsed-laser-modified-Si (M-Si) is mainly realized

J.-H. Zhao, X.-B. Li, Q.-D. Chen, and Z.-G. Chen are with the State Key Laboratory of Integrated Optoelectronics, College of Electronic Science and Engineering, Jilin University, Changchun 130012, China (e-mail: zhaojihong@jlu.edu.cn).

C.-H. Li is with the State Key Laboratory of Integrated Optoelectronics, College of Electronic Science and Engineering, Jilin University, Changchun 130012, China, and also with the Shenzhen Institutes of Advanced Technology, Chinese Academy of Sciences, Shenzhen 518055, China.

H.-B. Sun is with the State Key Laboratory of Integrated Optoelectronics, College of Electronic Science and Engineering, Jilin University, Changchun 130012, China, and also with the State Key Laboratory of Precision Measurement Technology and Instruments, Department of Precision Instrument, Tsinghua University, Beijing 100084, China (e-mail: hbsun@tsinghua.edu.cn).
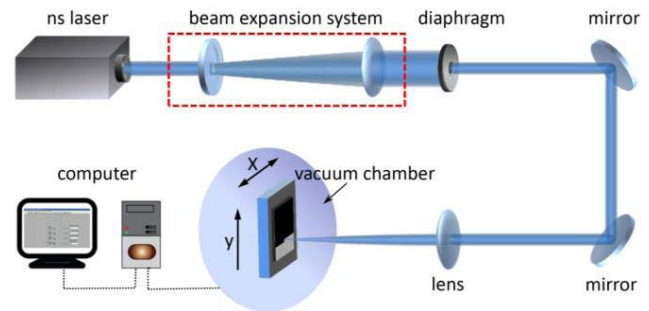
Fig. 1. Schematic of the experimental setup for the ns-laser processing system.

by the hyperdoping technique. For example, the chalcogen (sulfur, selenium, and tellurium)-doped Si materials from femtosecond (fs) lasers have been the focus of most investigations [8], [10], [11]. Although the chalcogen-doped Si photodiodes (PDs) fabricated with fs lasers show excellent photoresponses and high-gain characteristics to the light above the bandgap of crystalline Si, their photoresponse to the photoenergy below the bandgap is still unsatisfactory [18]–[20]. For one, there is a high concentration of impurities (10^{19}–10^{21} cm^{-3}) in the chalcogen-doped Si, and such doping can yield a large number of background free-carriers. As a result, a strong free-carrier absorption will contribute to the chalcogen-doped Si PD, which does not support photoelectric conversion. For another, there will be a strong ionized impurity scattering in the hyperdoped Si layer, which is also averse to the performance of the Si-based photodetector. To prevent the disadvantageous influence of hyperdoping on the photoelectric conversion of the device, this paper creates near-infrared (NIR) photodetectors based on a nanosecond (ns) laser M-Si produced in an argon (Ar) atmosphere. The photodetector shows perfect rectification characteristic and high above/below-bandgap photo response.

II. EXPERIMENTS

The schematic of the experimental setup is shown in Fig. 1. A frequency-tripled, Q-Switched, Nd:YAG ns laser (ns and Spectra-Physics) was used to fabricate M-Si samples. Here, the central wavelength, pulse duration, and repetition frequency of the ns laser were 355 nm, 10 ns, and 10 Hz, respectively. To obtain an energy density above the ablation threshold, a beam expanding system focused the uniform laser spot (laser power of 20 mW) with a 600 mm-lens onto an n-type Si substrate ($\rho = 4000\ \Omega\cdot$cm, $n_1 = 1.2 \times 10^{12}$ cm^{-3}). The diameter of the focused spot was estimated to be 180 μm. Then, the cleaned Si substrate was loaded into a vacuum

(a)

(b)
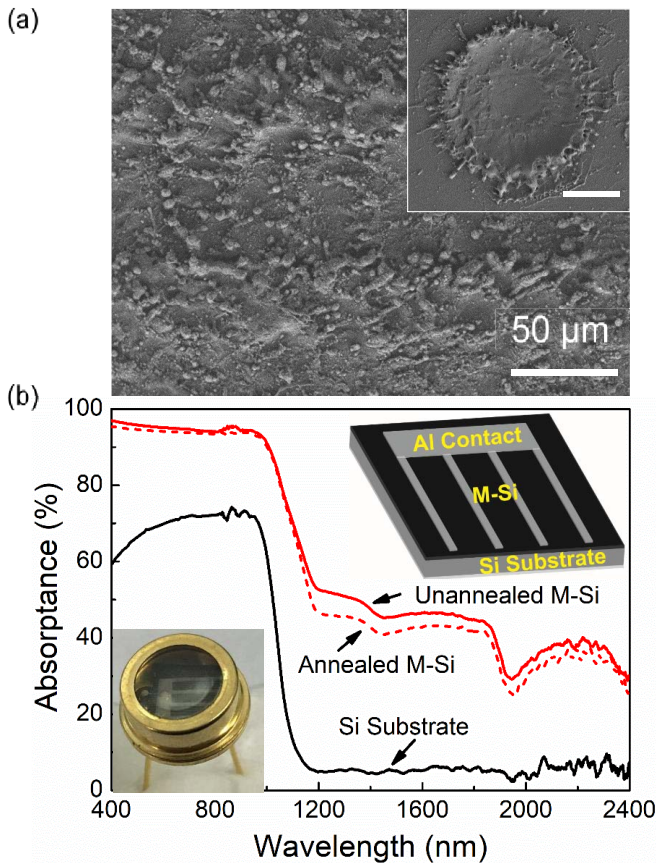

Fig. 2. (a) SEM image of the M-Si after line scanning. Inset: SEM image of a single spot exposure for the M-Si. The scale bar is 50 μm. (b) Absorptance of the M-Si sample before and after annealing and the absorptance of the unstructured Si substrate. Inset: schematic and the real image of the M-Si PD.

chamber filled with an Ar atmosphere (0.1 MPa) [21], which could be synchronously moved with the 2-D translation stage. The movement path of the sample was "S-line," and the moving speed was 250 μm/s. In addition, there was a 100 μm space between the two adjacent lines.

III. RESULTS AND DISCUSSION

The surface morphology of the M-Si sample [Fig. 2(a)] was measured by a field emission scanning electron microscope (SEM, JEOL JSM-7500F, and Japan). Due to the melting and resolidification process, the SEM image displays an obviously heating effect. Moreover, a certain amount of splashing can be clearly observed for the single spot exposure sample [Fig. 2(a) (inset)]. Fig. 2(b) shows the optical absorptance of the M-Si samples at wavelengths from 400 to 2400 nm, which was indirectly obtained by measuring the reflectance and transmittance of the sample using a spectrophotometer equipped with an integrating sphere (UV-3600 and LISR-UV3100). From Fig. 2(b), the M-Si samples indicate a strong broadband absorption. In particular, below-bandgap absorptance is significantly enhanced from the ns-laser irradiation. The large subbandgap absorptance (50.7% at 1310 nm) can be attributed to the Urbach states and the laser-induced structural defects (such as the di-vacancy V–V, multivacancy center, vacancy–oxygen complex, clusters of vacancy,
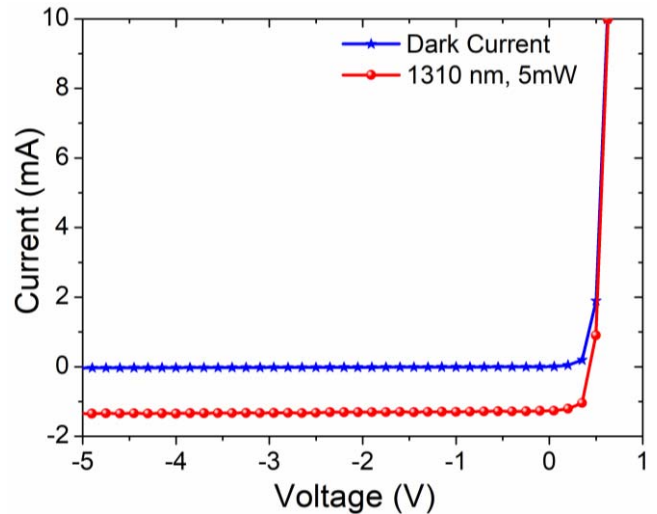

Fig. 3. Photo current and dark current versus voltage characteristics for the IR photodetector of the M-Si.

and vacancy-impurity associations) during the fast melt cooling process [22], [23]. The subbandgap absorption of the thermally annealed M-Si sample after 30 min at 873 K in an Ar atmosphere (annealing parameters apply to all annealed M-Si samples in this paper) slightly decreases (45.6% at 1310 nm). A small decrement of the light absorption below the bandgap contributes to the poor thermal stability of the small quantity Urbach states [24], [25]. The NIR photodetector was produced based on the stable light absorption below the bandgap of the M-Si.

The Hall effect measurement of the sheet carrier (electron) density of the annealed M-Si layer was 2.5×10^{13} cm^{-2}. The thickness of the ns-modified layer was estimated to be 500 nm [26], [27]. Thus, the carrier concentration could be calculated as 5×10^{17} cm^{-3} (n_2), which is five orders of magnitude higher than that of the Si substrate ($n_1 = 1.2 \times 10^{12}$ cm^{-3}). Finally, an NIR photodetector was produced based on the concentration difference of the carriers between the M-Si layer (N$^+$) and the Si substrate (N$^-$). The schematic of the NIR photodetector is shown in Fig. 2(b) (inset). The annealed M-Si sample with a 5×5 mm^2 square was cleaned with a dilute hydrofluoric acid solution (5%) before the thermal evaporation of aluminum (Al). The shape of the electrode in the M-Si surface (front electrode) is shown in Fig. 2(b) (inset); the unstructured Si backside was coated with an Al film (back electrode). Then, the metal electrodes were alloyed at 748 K for 1 min to form good Ohmic contacts between the metal Al film and the Si surface.

I–V characteristics of the N$^+$–N$^-$ junction between the M-Si layer and the Si substrate were taken with a Keithley 2410 sourcemeter (see Fig. 3). The N$^+$–N$^-$ junction exhibits perfect rectification characteristic, and the leakage current density of this device is 1.29×10^{-5} and 1.36×10^{-4} A · cm^2 at biases of -0.1 and -5 V, respectively. After illumination with an NIR source (laser diode, 1310 nm, 5 mW), the M-Si PD shows an obvious photoresponse and the responsivity (R) of 0.26 A/W at a bias of -5 V.

The M-Si photodetector has a higher room temperature responsivity in the broadband spectra from 400 to 1100 nm
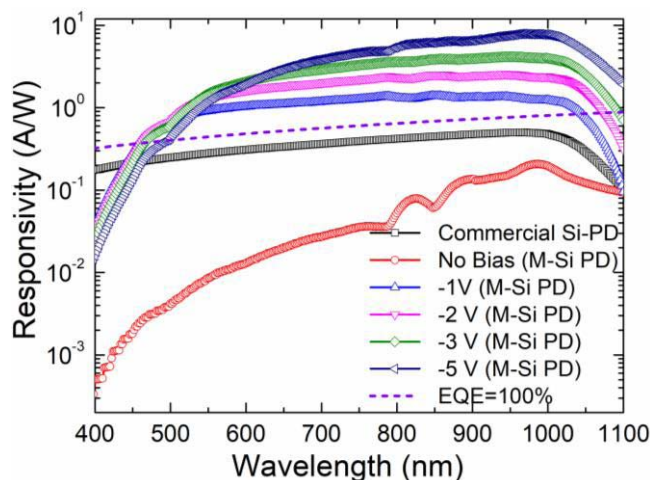
Fig. 4. Responsivity of the M-Si PD for several reverse biases. Responsivity of a commercial Si-PD is shown for reference. The EQE of 100% versus wavelength is shown as a short-dashed line.

Fig. 5. Time response of the M-Si PD to 900-nm IR light.

Fig. 6. Time response of the M-Si PD to 1310-nm IR light.

under a reverse bias. A white light 150-W Xenon lamp (7ILX150A-UVC) was passed through a monochromator and scanned from 400 to 1100 nm in increments of 2 nm. The illuminated area was approximately 5 mm × 3 mm and was placed to give the maximum photoresponse for the commercial Si PD and ns-laser-M-Si device. The white light was chopped so that the response could be measured using a lock-in amplifier (SR830). In the measurements, the monochromatic light was incident on the front side of the M-Si surface or the top surface of the commercial Si PD. The total incident optical power at each wavelength was measured using a commercial Si PD with a well-characterized response spectrum, and the highest intensity occurs at 960 nm. The external quantum efficiencies (EQEs) of 100% are given as the short-dashed line in Fig. 4, which shows the dependence of the photo responsivity on the reverse bias for an annealed M-Si PD. The responsivity of this M-Si PD is lower than that of the commercial Si PD at 0 V bias (no bias), and the responsivity of the M-Si PD at 960 nm is 0.17 A/W. However, the responsivity of this PD observably increases with the increase of the reverse bias ($R = 8$ A/W at -5 V, 960 nm). The EQE (1007% at -5 V bias, 960 nm) of this device is far higher than 100% when a reverse bias is applied. The M-Si PD still shows a gain ($R = 1.3$ A/W, EQE $= 160\%$ at 960 nm), even at a small reverse bias (-1 V). The gain mechanism could be attributed to the photoconductive gain. It is well-known that the carrier transit speed in the Si junction linearly or sublinearly increases with the increase of the reverse bias [28], [29]. In addition, the lifetime of the carriers could depend on the applied bias in the M-Si when the defect energy levels are introduced with the ns-laser irradiation [30], [31]. Also, the increased quantum efficiency may relate to the higher density of the defects and corresponding scattering processes inducing a high percentage of localized momentum changes of the carriers [32]. Thanks to the gain characteristic and high EQE, the M-Si device at a reverse bias has more important application than present commercial Si-PD in an NIR detection field.

Next, the response speed of the M-Si PD at 900-nm light illumination was carried out. The time response (rise time)
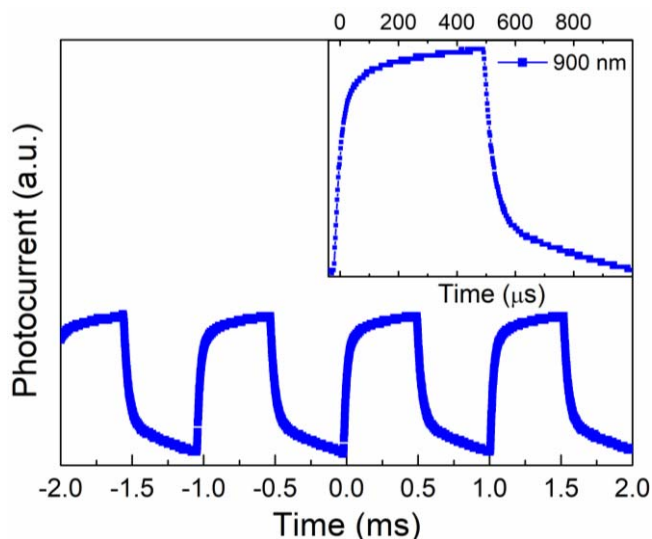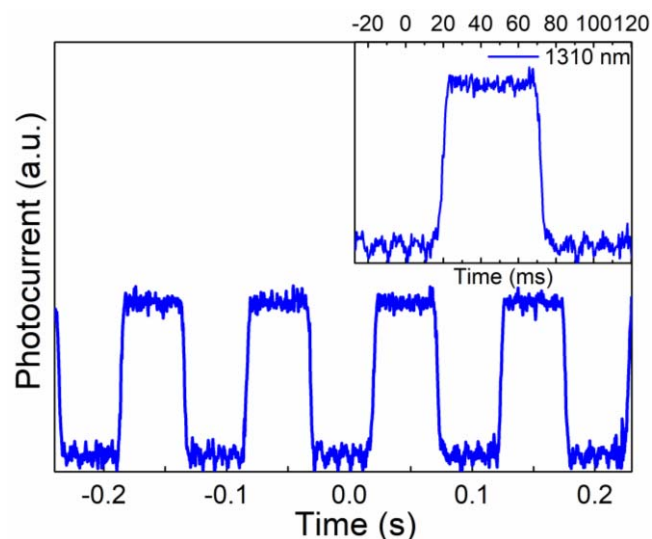
of the sample was obtained by measuring the voltage variation with the light signal being ON and OFF. The corresponding time response curve of the M-Si device to 900-nm light is shown in Fig. 5. The rise time is taken for the photocurrent to increase from 10% to 90% of its peak value. As demonstrated in Fig. 5 (inset), the rise time of the M-Si PD is determined to be 0.13 ms at 900 nm.

Similarly, the time response of the M-Si PD to 1310-nm light (photo energy below the bandgap of crystalline Si) was also measured and is shown in Fig. 6. The rise time is determined to be 3.6 ms based on Fig. 6 (inset). It is clear that the response speed of the M-Si to 1310-nm light is much slower than that of at 900 nm. Generally, the response speed of a Si photodetector is limited by a combination of three factors: diffusion of carriers, drift time in the depletion region, and capacitance of the depletion. Carriers generated outside the depletion region must diffuse to the junction, resulting in a considerable time delay. For the light illumination of 1310 nm, electron–hole (e–h) pairs can only be generated
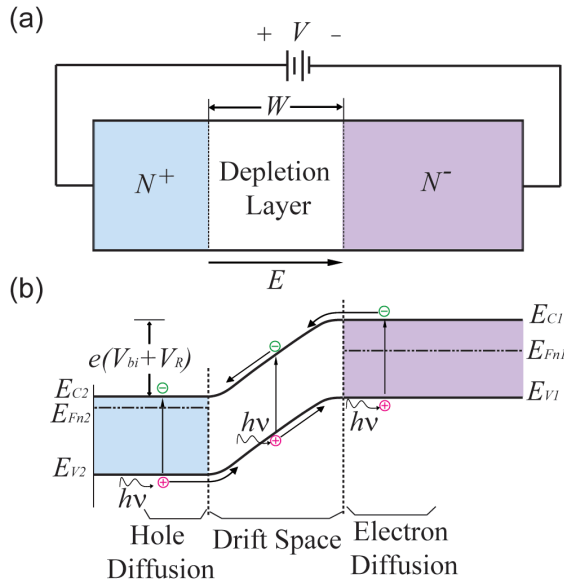
(a)

(b)

Fig. 7. (a) Cross-sectional view of N^+–N^- PD. (b) Energy-band diagram under reverse bias.

in the ns-laser-modified layer. In this case, the response time of the device is restricted by a slower diffusion speed in the M-Si from the imperfect crystalizing quality.

To understand the operation of the M-Si PD, the schematic representation of the N^+–N^- junction and the energy-band diagram under reverse-bias conditions are shown in Fig. 7. In Fig. 7, the E_{Ci}, E_{Vi}, and E_{Fi} represent the conduction band minimum (CBM), valence band maximum (VBM), and Fermi level, respectively, where $i = 1$ (for the N^- substrate) or 2 (for the N^+ M-Si layer). V_R (voltage across the depletion layer) should be smaller than the reverse-bias V in the external circuit because a large voltage is divided by the high-resistance Si substrate. The built-in potential V_{bi} can be estimated to be 0.34 V from the formula $V_{bi} = 0.026 \times \ln(n_2/n_1)$. The light absorption in the Si produces e–h pairs when a light beam is irradiated onto the M-Si surface. The e–h pairs produced in the depletion region or within a diffusion length will eventually be separated by the electric field E, leading to current flow in the external circuit as carriers drift across the depletion layer [33], [34]. The optical transition process occurs between the VBM and CBM for the photo above the bandgap energy, which is illustrated in Fig. 7. At this time, all the carriers in the N^+ layer and N^-–Si substrate can contribute to the photocurrent in the device. However, the photocurrent can only be generated in the M-Si layer for a photo below the bandgap energy. The subbandgap absorption in M-Si layer mainly comes from the Urbach states or laser-induced structural defects. By way of contrast, for the subbandgap absorption from Urbach states, the optical transition process occurs between Urbach tails; while for the laser-induced defects absorption, the optical transition process takes place between defects levels and band edge (VBM or CBM, it is dependent on levels position). At this moment, both the photocurrent and time response are limited by hole diffusion in the M-Si layer.

IV. CONCLUSION

In conclusion, the surface-M-Si IR photodetector was produced by ns-laser irradiation in an Ar atmosphere. The morphology of the melting and resolidification of Si shows an obvious heating effect from the ns-laser abla-tion. However, there still is a strong subbandgap absorption (45.6% at 1310 nm) after the annealing process, which is due to Urbach states and laser-induced structural defects. As a result, a bulk structure PD is produced based on the N^+–N^- junction formed between the M-Si layer and the Si substrate. This device shows perfect rectification characteristics and a high photoresponse to 1310 nm IR light, and a responsivity of 0.26 A/W is attained at a 5-V reverse bias. For light within the absorption limit, the photoresponse of the M-Si photodetector presents high-gain characteristics when a reverse bias is applied. For example, a responsivity of 8 A/W and an EQE of 1007% at a −5-V bias are obtained for 960-nm light. The high gain of this device under reverse bias is considered to be a photoconductor gain. Moreover, the time response of the M-Si PD has been demonstrated. The relatively slower rise time of the M-Si device for subbandgap photons is attributed to the slower diffusion speed of photogenerated e–h pairs in the laser-modified layer.

REFERENCES

[1] S. O. Kasap, *Optoelectronics and Photonics: Principles and Practices*. Upper Saddle River, NJ, USA: Prentice-Hall, 2001.
[2] Y. Kang *et al.*, "Monolithic germanium/silicon avalanche photodi-odes with 340 GHz gain–bandwidth product," *Nature Photon.*, vol. 3, pp. 59–63, Dec. 2008.
[3] J. J. Ackert *et al.*, "High-speed detection at two micrometres with mono-lithic silicon photodiodes," *Nature Photon.*, vol. 9, no. 6, pp. 393–396, 2015.
[4] P. Lecoy, B. Delacressonniere, and D. Pasquet, "SiGe heterojunc-tion bipolar phototransistor for optics–microwaves interfacing," *Int. J. Microw. Wireless Technol.*, vol. 3, no. 6, pp. 633–636, 2011.
[5] K. Xu *et al.*, "Light emitting devices in Si CMOS and RF bipolar integrated circuits," *LEUKOS, J. Illum. Eng. Soc.*, vol. 12, no. 4, pp. 203–212, 2016.
[6] K. Xu, "Integrated silicon directly modulated light source using p-well in standard CMOS technology," *IEEE Sensors J.*, vol. 16, no. 16, pp. 6184–6191, Aug. 2016.
[7] S. Villa, A. L. Lacaita, L. M. Perron, and R. Bez, "A physically-based model of the effective mobility in heavily-doped n-MOSFETs," *IEEE Trans. Electron Devices*, vol. 45, no. 1, pp. 110–115, Jan. 1998.
[8] C. Wu *et al.*, "Near-unity below-band-gap absorption by microstructured silicon," *Appl. Phys. Lett.*, vol. 78, no. 13, p. 1850, 2001.
[9] R. Younkin, J. E. Carey, E. Mazur, J. A. Levinson, and C. M. Friend, "Infrared absorption by conical silicon microstructures made in a variety of background gases using femtosecond-laser pulses," *J. Appl. Phys.*, vol. 93, no. 5, pp. 2626–2629, 2003.
[10] B. R. Tull, M. T. Winkler, and E. Mazur, "The role of diffusion in broadband infrared absorption in chalcogen-doped silicon," *Appl. Phys. A, Solids Surf.*, vol. 96, no. 2, pp. 327–334, 2009.
[11] M. Tabbal, T. Kim, D. N. Woolf, B. Shin, and M. J. Aziz, "Fabrication and sub-band-gap absorption of single-crystal Si supersaturated with Se by pulsed laser mixing," *Appl. Phys. A, Solids Surf.*, vol. 98, no. 3, pp. 589–594, 2010.
[12] M.-J. Sher and E. Mazur, "Intermediate band conduction in femtosecond-laser hyperdoped silicon," *Appl. Phys. Lett.*, vol. 105, no. 3, p. 032103, 2014.
[13] X. Dong *et al.*, "A nitrogen-hyperdoped silicon material formed by femtosecond laser irradiation," *Appl. Phys. Lett.*, vol. 104, p. 091907, Feb. 2014.
[14] Y. Peng *et al.*, "Annealing-insensitive 'black silicon' with high infrared absorption," *J. Appl. Phys.*, vol. 116, no. 7, p. 073102, 2014.

[15] X.-Y. Yu, J.-H. Zhao, C.-H. Li, Q.-D. Chen, and H.-B. Sun, "Gold-hyperdoped black silicon with high IR absorption by femtosecond laser irradiation," *IEEE Trans. Nanotechnol.*, vol. 16, no. 3, pp. 502–506, May 2017.

[16] C.-H. Li, J.-H. Zhao, Q.-D. Chen, J. Feng, and H.-B. Sun, "Sub-bandgap photo-response of non-doped black-silicon fabricated by nanosecond laser irradiation," *Opt. Lett.*, vol. 43, no. 8, pp. 1710–1713, 2018.

[17] C.-H. Li *et al.*, "Black silicon IR photodiode supersaturated with nitrogen by femtosecond laser irradiation," *IEEE Sensors J.*, vol. 18, no. 9, pp. 3595–3601, May 2018.

[18] J. E. Carey, C. H. Crouch, M. Shen, and E. Mazur, "Visible and near-infrared responsivity of femtosecond-laser microstructured silicon photodiodes," *Opt. Lett.*, vol. 30, no. 14, pp. 1773–1775, 2005.

[19] Z. Huang, J. E. Carey, M. Liu, X. Guo, E. Mazur, and J. C. Campbell, "Microstructured silicon photodetector," *Appl. Phys. Lett.*, vol. 89, p. 033506, Jul. 2006.

[20] M. U. Pralle *et al.*, "IR CMOS: Ultrafast laser-enhanced silicon detection," *Proc. SPIE*, vol. 8012, p. 801222, May 2011.

[21] R. J. Younkin, "Surface studies and microstructure fabrication using femtosecond laser pulses," Ph.D. dissertation, Dept. Division Eng. Appl. Sci., Harvard Univ., Cambridge, MA, USA, 2001.

[22] A. Barhdadi, B. Hartiti, and J.-C. C. Müller, "Active defects generated in silicon by laser doping process," *African Rev. Phys.*, vol. 6, p. 229, Oct. 2012.

[23] L. Mandel, E. C. G. Sudarshan, and E. Wolf, "Theory of photoelectric detection of light fluctuations," *Proc. Phys. Soc.*, vol. 84, p. 435, Sep. 1964.

[24] X.-B. Li, X. Q. Liu, X. D. Han, and S. B. Zhang, "Role of electronic excitation in phase-change memory materials: A brief review," *Phys. Status Solidi B*, vol. 249, no. 10, pp. 1861–1866, 2012.

[25] C.-H. Li, J.-H. Zhao, Q.-D. Chen, J. Feng, W.-T. Zheng, and H.-B. Sun, "Infrared absorption of femtosecond laser textured silicon under vacuum," *IEEE Photon. Technol. Lett.*, vol. 27, no. 14, pp. 1481–1484, Jul. 15, 2015.

[26] M. J. Smith, Y. T. Lin, M. J. Sher, M. T. Winkler, E. Mazur, and S. Gradečak, "Pressure-induced phase transformations during femtosecond-laser doping of silicon," *J. Appl. Phys.*, vol. 110, no. 5, p. 053524, 2011.

[27] M.-J. Sher, M. T. Winkler, and E. Mazur, "Pulsed-laser hyperdoping and surface texturing for photovoltaics," *MRS Bull.*, vol. 36, no. 6, pp. 439–445, 2011.

[28] C. Jacoboni, C. Canali, G. Ottaviani, and A. A. Quaranta, "A review of some charge transport properties of silicon," *Solid-State Electron.*, vol. 20, pp. 77–89, Feb. 1977.

[29] K. Xu, "Monolithically integrated Si gate-controlled light-emitting device: Science and properties," *J. Opt.*, vol. 20, p. 024014, Jan. 2018.

[30] A. Chantre, "Introduction to defect bistability," *Appl. Phys. A, Solids Surf.*, vol. 48, no. 1, pp. 3–9, 1989.

[31] R. Czaputa, "Transition metal impurities in silicon: New defect reactions," *Appl. Phys. A, Solids Surf.*, vol. 49, no. 4, pp. 431–436, 1989.

[32] K. Xu *et al.*, "Light emission from a poly-silicon device with carrier injection engineering," *Mater. Sci. Eng. B*, vol. 231, pp. 28–31, May 2018.

[33] D. A. Neamen, *Semiconductor Physics and Devices*, 3rd ed. New York, NY, USA: McGraw-Hill, 2002, pp. 634–638.

[34] S. M. Sze, *Physics of Semiconductor Devices*, 2nd ed. Hoboken, NJ, USA: Wiley, 1981, pp. 749–754.

Chun-Hao Li received the B.S. and Ph.D. degrees from the College of Electronic Science and Engineering, Jilin University, Changchun, China, in 2012 and 2018, respectively.

He is currently a Post-Doctoral Researcher with the Shenzhen Institutes of Advanced Technology, Chinese Academy of Sciences, Shenzhen, China. His current research interests include ultrafast laser micro- and nano-fabrication.

Xian-Bin Li received the B.S., M.S., and Ph.D. degrees from Jilin University, Changchun, China, in 2005, 2007, and 2010, respectively.

He is currently an Associate Professor with the College of Electronic Science and Engineering, Jilin University. His current research interests include the key problems in microelectronics and optoelectronics with the first principles calculation, including phase-change memory physics, semiconductor defect physics, and 2-D semiconductor design.

Qi-Dai Chen received the B.S. degree in physics from the University of Science and Technology of China, Hefei, China, in 1998, and the Ph.D. degree from the Institute of Physics, Chinese Academy of Sciences, Beijing, China, in 2004.

He is currently a Professor with Jilin University, Changchun, China. His current research interests include laser microfabrication, ultrafast laser spectroscopy, and photophysics.

Zhan-Guo Chen received the B.S., M.S., and Ph.D. degrees from the College of Electronic Science and Engineering, Jilin University, Changchun, China, in 1994, 1997 and 2002, respectively.

He is currently a Full Professor with Jilin University. His research interests include wide-bandgap semiconductors and silicon optoelectronics.

Ji-Hong Zhao received the B.S. and Ph.D. degrees from the College of Electronic Science and Engineering, Jilin University, Changchun, China, in 2006 and 2011, respectively.

She is currently an Associate Professor with Jilin University. Her current research interests include analysis of properties of semiconductor surface by nonlinear optics, femtosecond laser micro- and nano-fabrication, and doping of semiconductors by femtosecond laser.

Hong-Bo Sun (M'99–SM'17–F'18) received the B.S. and Ph.D. degrees in electronics from Jilin University, Changchun, China, in 1992 and 1996, respectively.

His current research interests is ultrafast and nano-photonics. He is an Executive Editor-in-Chief of *Light: Science and Applications* (Nature Publishing Group), and an Editor of *Optics Letters*.